Space-charge spectroscopy of self-assembled Ge-rich dots on Si grown by MBE

K. Schmalz
Institute for Semiconductor Physics, Walter-Korsing-Strasse 2, 15230 Frankfurt (Oder), Germany

I. N. Yassievich
Ioffe Physico-Technical Institute, Polytechnicheskaya 26, 194021 St. Petersburg, Russia

P. Schittenhelm and G. Abstreiter
Walter Schottky Institut, TU München, Am Coulombwall, 85748 Garching, Germany
(Received 1 September 1998)

The results of deep-level transient spectroscopy and admittance measurements of self-assembled Ge-rich dots are presented. The investigated quantum well (QW) Ge-rich layers in silicon consist of a thin-wetting QW layer with a width of 4–4.5 monolayers and three-dimensional dots (islands), with heights of about 6–8.5 nm and lateral dimensions of about 190–250 nm. Good agreement was observed with photoluminescence data. An enhancement of the lateral hole transport between the islands via the wetting layer due to thermally activated tunneling was observed. This effect is explained by a strong lateral electric field, which is induced by Coulomb charge of confined holes in the disc-shaped islands. [S0163-1829(99)03516-X]

I. INTRODUCTION

Self-assembled Stranski-Krastanov growth of dots in semiconductor heterostructures has recently attracted strong interest, both in strained III-V material[1–3] and IV-IV heterostructures.[4–9] Novel devices based on Ge dots grown on a Si substrate have been already proposed.[10] Recently, several publications have reported on different characterization techniques to investigate the structural[4,5,9,11] and optical[7,8,10,12] properties of Ge and SiGe dots on Si.

In this paper, we present space-charge spectroscopy analysis of self-assembled Ge-rich dots embedded in Si: Space-charge spectroscopy techniques, such as admittance spectroscopy, deep-level transient spectroscopy (DLTS), and capacitance voltage measurements (CV), have been used with increasing success to study quantum well (QW) structures.[12–15] However, there are only a few reports on the application of space spectroscopy to investigate QW structures with islands.

A DLTS study is reported for coherently grown InP islands embedded in $Ga_{0.5}In_{0.5}P$ layer.[13] The islands are randomly distributed and the density of the dots is about $2\times10^9\,cm^{-2}$, and their dimensions are 13 nm in height and about 40 nm in the lateral dimension. A decrease of the activation energy from 230 meV to about 180 meV with increasing electron concentration in the islands, was interpreted in terms of Coulomb charging of the quantum dots. DLTS results have also been published for chemical vapor deposition (CVD) grown, *p*-type $Si/SiGe_{0.7}Ge_{0.3}/Si$ QW structures with 5–15-nm thick islands, where the SiGe layer thickness between the islands is uniform and less than 2 nm thick.[12] The average distance between the islands was about 300 nm. The decrease of the activation energy from 238 to 97 meV with increasing hole concentration in the islands was explained by a broad distribution of confinement energies due to the different thicknesses of the SiGe layer between the islands and in the islands.

Recently, a photoluminescence study of the crossover from two-dimensional to three-dimensional growth for Ge on Si(100) has been published, demonstrating island formation as a function of the monolayer (ML) Ge deposition.[9–11] For samples containing 6 ML Ge, only a low concentration of islands ($2\times10^8\,cm^{-2}$) of nearly uniform size, approximately 150 nm in diameter and 15 nm in height, was observed. An additional confinement due to the lateral size of the islands was not expected, because the island diameter was relatively large. For samples with Ge layer thickness of 12 ML, a decreasing confinement in the growth direction was observed as the thickness of the islands increased by a factor of 3 as the layer thickness was increased from 5 to 12 ML. Additional photoluminescence lines that are redshifted with respect to the photoluminescence signal of the two-dimensional strained layers were attributed to islands formed by three-dimensional growth.[8,9,10] The occurrence of these new lines was accompanied by a blueshift of the photoluminescence of the two-dimensional layers, indicating a strong Ge diffusion from the two-dimensional layers towards the islands.

The aim of this paper is to study the hole emission processes for such *p*-type Si/Ge/Si structures with islands under equilibrium and nonequilibrium conditions realized in admittance spectroscopy and DLTS investigations, and to clarify the peculiarities of hole emission from the islands. Our experimental study combines admittance, DLTS, and PL investigations for molecular-beam epitaxy (MBE) grown Si/Ge/Si structures with islands, for which the Ge deposition thickness was varied from 4 to 12 ML.

DLTS is a standard technique for measuring the activation energy of carrier emission from deep levels. In applying DLTS for studying carrier emission from quantum well (QW) structures the main problem is induced by the lateral diffusion of confined carriers, leading to the situation that the carriers could be swept from the QW region beneath the Schottky contact laterally before hole emission across the

barrier can occur. Direct hole emission from $Si/Si_{1-x}Ge_x/Si$ QW structures was observed for narrow QW's (2–3 nm) with high-Ge concentration ($x=0.3-0.5$),[15] because here alloy and interface scattering decrease hole mobility, and therefore, it was easier to observe direct hole emission.

The activation energy E_a of conductance across the QW can be obtained using admittance spectroscopy.[14,15] If the SiGe layer is undoped, the activation energy E_a is well approximated by $E_a=\Delta E_v-E_1$, where ΔE_v is the valence-band offset and E_1 is the confinement energy of the first level of the heavy hole in the QW.[14] The activation energies of hole emission, determined by admittance spectroscopy for equilibrium conditions, and measured by DLTS under low-electric field and for higher nonequilibrium hole concentration are in good agreement.[15]

A low-hole mobility is also expected for Si/Ge/Si structures with Ge-rich islands, allowing hole emission to be studied by DLTS. In the case of DLTS, the confined hole concentration can be changed in the QW layer by the reverse bias applied to the structure. We obtained the activation energy of hole emission from the islands as a function of hole concentration. This allows us to characterize the effective band offset and an effective density of states for the Ge-rich islands as function of the activation energy. The activation energy of hole emission from the Ge layer between the Ge-rich islands was measured by admittance spectroscopy, which allows us to characterize the effective band offset for this Ge layer.

We obtained the band offsets for the Ge-rich islands and for the Ge layer between the islands, respectively, also by photoluminescence (PL) measurements.

The theoretical part of this paper deals with a detailed analysis of the effect of thermally activated lateral tunneling for the investigated Ge-rich islands due to a strong lateral electric field. The paper is organized as follows. Section II describes sample preparation and gives the results of PL measurements and structural investigations. In Sec. III, we present the results of admittance spectroscopy and DLTS. Section IV discusses the experimental results.

II. EXPERIMENT

A series of samples with Ge-rich dots was grown on Si(100) substrates, B-doped, with a resistivity of 0.01–0.02 Ω cm in a commercial solid source Riber Siva 32 MBE using electron beam evaporators for Si and Ge. On a 200-nm thick *p*-type Si buffer with a boron doping of $10^{17}\,cm^{-3}$, layers of different Ge coverage, ranging from 4 monolayers (ML) to 12 ML were embedded between 30 nm of undoped Si spacer layers (Fig. 1). Finally, the structure was covered with a 300-nm thick *p*-type Si cap, also $10^{17}\,cm^{-3}$ boron doped. Details of growth and sample preparation have been reported elsewhere.[9]

The growth parameters, the height, diameter, and surface density of the dots as received from reference samples by transmission electron microscopy and atomic force microscopy[10,11] are summarized in Table I. The values marked with an asterisk in Table I are received from multilayer samples and may differ somewhat from those for the single-layer structures analyzed in this communication.

Schottky diodes were prepared by W/Ti deposition followed by Al or Pt deposition. The effective area of the Schottky contact was $A=1.3\times10^{-2}\,cm^{-2}$. For the CV and DLTS investigations, we also used structures for which the thickness of the cap layer was reduced by chemically etching. We used a mesa Schottky diode geometry (Fig. 1).

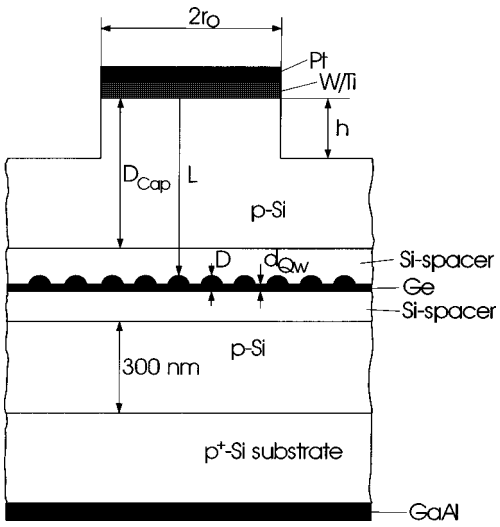

FIG. 1. Schematic picture of the mesa WTi Schottky diode geometry used.

The deep-level transient spectroscopy (DLTS) measurements were performed with a commercial DLTS spectrometer (DLS-82 from SEMILAB, Hungary), and CV and admittance investigations were carried out using the impedance analyzer HP 4192A. Details of photoluminescence (PL) measurements are described elsewhere.[8] PL results of the investigated samples are presented in Table II.

III. SPACE-CHARGE SPECTROSCOPY RESULTS

In this section, we present experimental results on the hole thermal emission rate, obtained for narrow Si/Ge/Si layer structures with islands at equilibrium and nonequilibrium conditions.

A. Capacitance voltage and admittance spectroscopy measurements

We begin with capacitance voltage (CV) and admittance spectroscopy measurements, which give the apparent carrier concentration profile and the activation energy of hole emission under equilibrium conditions. The dependence of the capacitance C on the reverse bias U_R was obtained from CV measurements performed at 1 MHz. The depth profiles of the apparent carrier concentration $N=N(W)$ obtained from the dependence $C=C(U_R)$ at different temperatures are shown in Fig. 2 for the structure with 4 ML Ge deposition. The $N(W)$ profiles for this sample give nearly constant acceptor concentrations N_{A1} and N_{A2} of about $10^{17}\,cm^{-3}$ in the boron-doped cap and buffer layers above and below the Ge layer, respectively. A concentration peak appears in the $N(W)$ profile in the region of the Ge layer, which is expected for hole confinement in the QW.[14]

For the Si/Ge/Si structures with 300-nm thick cap layers and an acceptor concentration in the cap layer of about $10^{17}\,cm^{-3}$, the Ge layer is located outside the Schottky

TABLE I. Growth parameters, height, diameter, and surface density of islands obtained from reference samples by transmission electron microscopy.

Sample	ML	Growth Temperature	Growth Rate [Å/s]	Dot Height [nm]	Dot Diameter [nm]	Dot Density [μm^{-2}]
*R*1	4	740	0,2			
*R*2	5	740	0,2		190	0,36
*R*3	6	740	0,2	6	190	9,3
*R*4	12	740	0,2	8.5	250	30
*R*5	5	670	0,075	7	180*	4

depletion region at zero bias ($U_R = 0$ V). From the equivalent circuit for the space-charge region of the Schottky diode and the QW, one obtains C_p and G_p (capacitance C and conductance G measured in a parallel equivalent circuit) as a function of C_1, C_2, G, and $\omega = 2\pi f$, where C_1 is the capacitance of the space-charge region of the Schottky diode, C_2 the capacitance of the QW, and G the conductance across the QW.[14] A maximum in the temperature dependence $G_p(T)$ of the conductance appears at $G^* = 2\pi f(C_1 + C_2)$.

The temperature dependence of the conductance G of the QW is given by $G(T) \sim T^{1/2} \exp(-E_a/k_B T)$. Hence, the activation energy E_a is estimated from the Arrhenius plot of the measurement frequency f versus the temperature, at which the conductance peak occurs. The activation energy E_a is well approximated by the potential barrier $E_a = \Delta E_v - E_1$, where ΔE_v is the valence-band offset and E_1 is the confinement energy of the first level of the heavy hole in the QW.[14] In case of Si/Ge/Si structures with islands, the conductance across the Ge layer is dominated by the lowest potential barrier at the Ge layer. Thus, in case of Si/Ge/Si structures with islands, the measured activation energy corresponds to the potential barrier at the wetting layer between the islands.

Figure 3 shows the capacitance C and conductance G measured in the parallel equivalent circuit as a function of temperature for a structure with 4 ML deposition. The steplike change in $C(T)$ and the corresponding peak in $G(T)$ indicate hole confinement in the Ge layer. In Fig. 4, Arrhenius plots of the measurement frequency f are presented for structures with different Ge layer deposition thicknesses. The values of the activation energy E_a for the investigated structures obtained from the Arrhenius plot are presented in Table II.

B. DLTS measurements

The DLTS results give the dependence of the activation energy of hole emission on the hole concentration. We obtained the minimum reverse bias U_R^* at which the Ge layer becomes depleted from the $C = C(U_R)$ dependences measured at various temperatures.[15] For this condition, we performed DLTS measurements. A strong DLTS signal of peak amplitude $\Delta C/C$, related to hole emission from the QW, was observed for Si/Ge/Si structures with 12 (Fig. 5), 6, and 5 ML Ge deposition, respectively, but not for those with 4 ML Ge deposition. We assume that this is due to lateral hole diffusion in the Ge QW layer without islands,[15] i.e., with 4 ML Ge deposition. Better conditions for DLTS investigations are realized for the structures with islands in the Ge layer. In this case, holes are localized in the islands due to the deeper energy state.

The DLTS peak shape was observed to depend strongly on the pulse bias U_1. For larger pulse amplitudes ($U_R^* - U_1$), the DLTS peak broadens on the low-temperature side. Figure 5 demonstrates this effect for the structure with 12 ML deposition. This broadening is very similar to that observed for *p*-type $Si/Si_{0.7}Ge_{0.3}/Si$ structures with islands,[16] but different from the broadening induced by a decay of nonequilibrium hole concentration due to hole transport in the QW plane.[15] This problem will be discussed in detail in the following section.

To measure the distribution of activation energies for hole emission, we changed the reverse and the pulse biases in order to have a constant bias difference $\Delta U = U_R - U_1$ ($= 0.4$ V). Sharp peaks were observed in the DLTS spectrum (Fig. 6). Figure 7 shows the Arrhenius plots of the hole emission rate e_p for a Si/Ge/Si structure (12 ML Ge deposition)

TABLE II. Results of photoluminescence, admittance spectroscopy and deep-level transient transient spectroscopy measurements for *p*-type Si/Ge/Si structures with different ML Ge deposition (E_g is the energy gap of Si and E_{NP} is the photon energy for no-phonon line, $E^{Admittance}$ the activation energy measured by admittance spectroscopy, E^{DLTS} the activation energy measured by deep-level transient spectroscopy).

Sample	ML	E_g-E_{NP} for wetting layer (meV)	$E^{Admittance}$ for wetting layer (meV)	E_g-E_{NP} for islands (meV)	E^{DLTS} for islands (meV)
*R*1	4	79	44		
*R*2	5	101	56	218	
*R*3	6	89	51	225	285
*R*4	12		48	251	300
*R*5	5	111	64	223	230

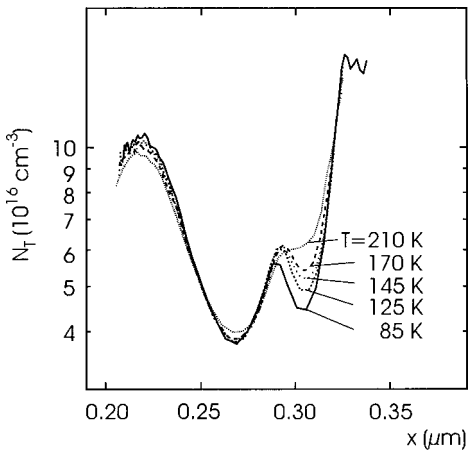

FIG. 2. Apparent carrier concentration profile $N=N(W)$ obtained from 1-MHz CV measurements at different temperatures for p-type Si/Ge/Si structures with 4 ML Ge deposition.

with various nonequilibrium hole concentrations n_w^*, realized by various reverse bias U_R and pulse bias amplitudes U_1. The activation energies E_a decreases from 300 meV down to 46 meV with increasing hole concentration. Note, that the activation energy E_a, observed by DLTS for large hole concentrations n_w^*, is in good agreement with the value of E_a obtained by admittance spectroscopy. In this case, the activation energy is controlled by the potential barrier at the wetting layer between the islands.

The hole concentration n_w^*, which is emitted from the QW with activation energy E_a was estimated from the DLTS signal $\Delta C/C$ through the relation $n_w^* = (\Delta C/C)(2N_A W^2/L)$, with $\Delta C/C$ at the measurement frequency $f=2500\,\mathrm{s}^{-1}$. Here, N_A is the acceptor concentration in the buffer, L is the thickness of the Si layer between the Schottky contact and the Ge layer, and W is the width of the depletion region. Using the dependence $n_w^*(E_a)$, we can calculate the effective density of states $N(E)=dn_w^*/dE_a$ as a function of the activation energy.

$N(E)$ was obtained from the experimental results by the relation $N(E)=n_w^*/(0.48k_BT)$, previously reported for the

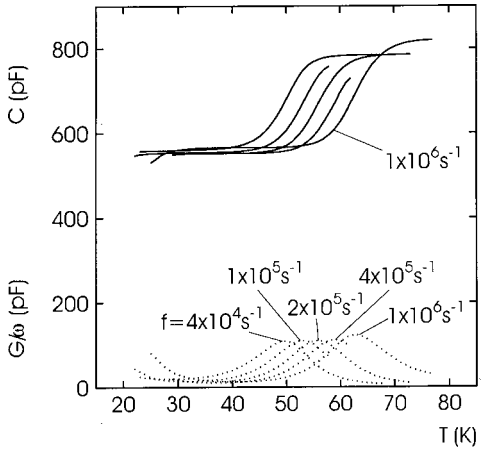

FIG. 3. Temperature dependence of the capacitance C (upper panel) and the normalized conductance G/ω (lower panel) for a measurement frequency $f=1$ MHz for a p-type Si/Ge/Si structure with 4 ML deposition.

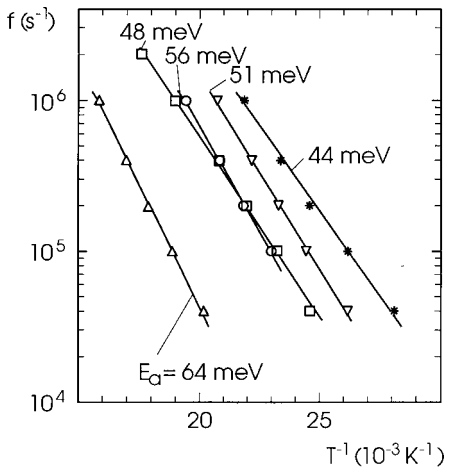

FIG. 4. Arrhenius plots of the normalized frequency $f/T^{1/2}$ of the conductance peak for p-type Si/Ge/Si structures with different Ge ML deposition. (Sample $R1$—*, $R2$—○, $R3$—∇, $R4$—□, $R5$—△). The measurements were performed at $U_R=0.2$ V.

DLTS characterization of an interface state distribution.[17] The factor 0.48 is due to signal averaging by lock-in detection.[17] The energy E is taken as $E=E_a$. The effective density of states $N(E_a)$ is drawn in Fig. 8 for Si/Ge/Si structures with different Ge layer depositions.

IV. DISCUSSION

The Ge-rich QW layers consist of a thin-wetting QW layer of 4–4.5 ML width and three-dimensional dots (islands) with heights d (in z direction) of about 6–8.5 nm and lateral dimensions D (in xy plane) of about 190–250 nm. These islands are thus too large to induce lateral quantum confinement. We can approximate the islands by a quantum well in the z direction (Fig. 9). Previous studies demonstrate strain-relaxed islands with Ge content about 70–90 % for the growth conditions used.[9–11] To discuss the results of space charge spectroscopy, it is necessary to take into account the potential barriers induced by holes confined on the boundary

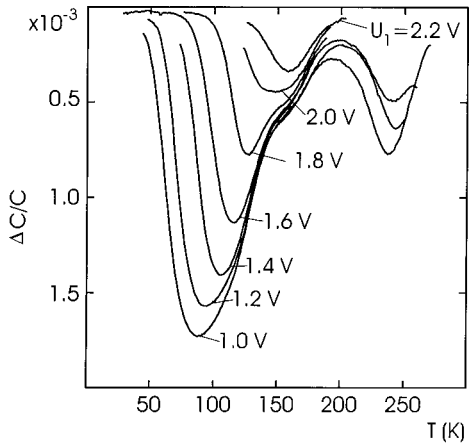

FIG. 5. Deep-level transient spectroscopy spectrum of p-type Si/Ge/Si structures with islands (12 ML Ge deposition) measured at the reverse bias $U_R=3$ V and the pulse frequency $f=2500\,\mathrm{s}^{-1}$ (corresponding to emission rate window $e_0=5580\,\mathrm{s}^{-1}$) for different pulse biases U_1 with pulse duration 5 μs.

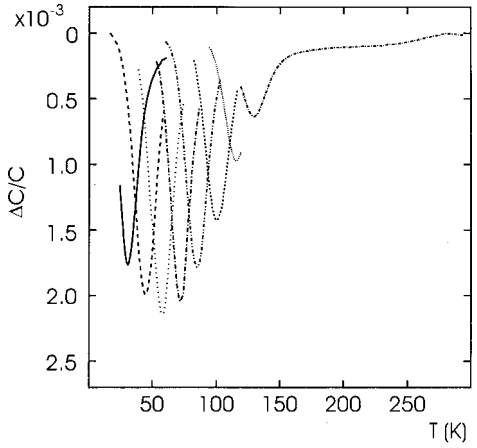

FIG. 6. Deep-level transient spectroscopy spectrum of *p*-type Si/Ge/Si structures with islands (12 ML Ge deposition) measured at different reverse bias U_R and pulse bias U_1 with the bias difference $\Delta U = U_R - U_1 = 0.4$ V. The pulse frequency is $f = 2500\,s^{-1}$ (corresponding to emission rate window $e_0 = 5580\,s^{-1}$) and the pulse duration 5 μs. [$U_R = 1.0$ V (straight), 1.2 V (dashed), 1.4 V (dotted), 1.6 V, 1.8 V, 2.0 V, 2.2 V, 2.4 V].

of the wetting layer and the Ge-rich islands.

A summary of the data obtained by photoluminescence and by space-charge spectroscopy are presented in Table II. Admittance spectroscopy results for the activation energy are in good agreement with PL data for $E_g - E_{NP}$ for the wetting layers. (E_g is the energy gap of silicon and E_{NP} is the photoluminescence energy for the no-phonon line[9]), which should correspond to $E_{vw} - E_{1w}$ (E_{vw} and E_{1w} are the band offset relative to Si and the space quantization level in the wetting QW layer, respectively). However, all data obtained by admittance spectroscopy are about 30–40 meV smaller than the corresponding PL data. This difference can be explained first by an exciton effect provided the increase of the

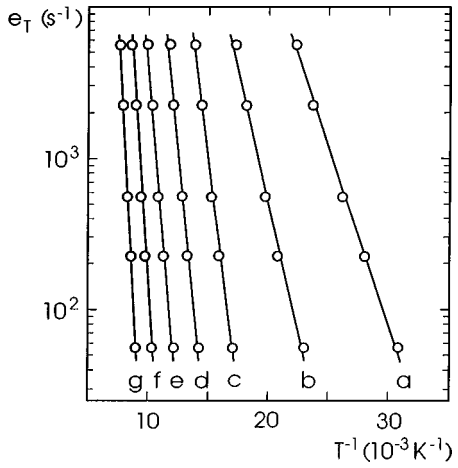

FIG. 7. Arrhenius plots of the hole emission rate e_p for a *p*-type Si/Ge/Si structure with islands (12 ML Ge deposition) measured at different reverse bias U_R and pulse bias U_1 with $U_R - U_1 = 0.4$ V. The pulse duration is 5 μs. The parameter is the reverse bias U_R leading to the following activation energy E_a. (a) $U_R = 2.4$ V, $E_a = 300$ meV; (b) $U_R = 2.2$ V, $E_a = 241$ meV; (c) $U_R = 2.0$ V, $E_a = 189$ meV; (d) $U_R = 1.8$ V, $E_a = 162$ meV; (e) $U_R = 1.6$ V, $E_a = 125$ meV; (f) $U_R = 1.4$ V, $E_a = 69$ meV; (g) $U_R = 1.2$ V, $E_a = 46$ meV.

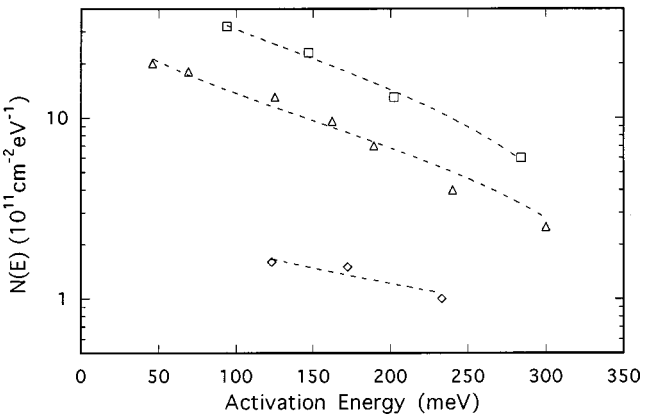

FIG. 8. The effective density of states $N(E_a)$ as function of the activation energy E_a for *p*-type Si/Ge/Si structures with different Ge ML deposition: ◇—5 ML, □—6 ML, △—12 ML.

exciton binding energy due to space quantization is taken into account. This effect is rather large also in the case of ultrathin QW layers, as demonstrated for ultrathin InAs layers in GaAs,[18] where a binding energy of the exciton was observed to be about two times larger than in the bulk. Second, it has been shown that thermally activated tunneling via potential barriers can decrease the activation energy deduced from admittance spectroscopy.[15]

The maximum values of the activation energy measured by DLTS are about 50 meV larger than the values estimated from the position of the PL peak. However, the PL peak is broadened by about 50 meV on both sides, presumably due to a size distribution of islands. PL results for structures with the same growth conditions as used in our study are given in Ref. 8. But, the maximum activation energy measured by DLTS corresponds to islands with the largest potential barriers for holes. One may therefore conclude that these is reasonable.

The DLTS results show a decreasing activation energy with increasing concentration of confined holes. This result is shown Fig. 8, where the effective density of states $N(E) = dn_w^*/dE_A$ obtained from the DLTS signal is presented. The hole concentration in an island as function of activation energy E_A^* can be obtained by integration on dn_w^*/dE_A with respect to the activation energy E_A^*, and taking into account the effective density of islands ρ and the island area A, i.e.,

$$n_{dw} = A\rho \int_0^{E_A^*} N(E_a)\,dE_a\,. \tag{1}$$

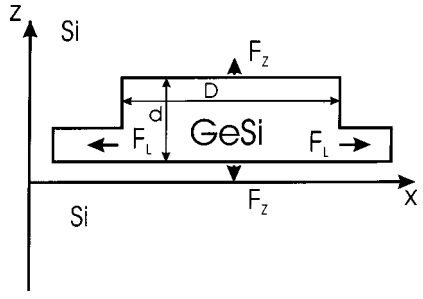

FIG. 9. Schematic picture of the Ge islands. The lateral and vertical electric fields are indicated.

A similar behavior of activation energy was previously observed for InP islands embedded in $Ga_{0.5}In_{0.5}P$ layer[13] and interpreted in terms of Coulomb charging of quantum dots. It was also observed for CVD-grown SiGe islands,[12,16] where the broad distribution of confined energies was explained by a broad distribution of island sizes.

In our case, the broadening in the PL line is about 100 meV, but we observed in the DLTS study a continuous increase of the activation energy from about 50 meV to about 300 meV with decreasing confined hole concentration. Thus, this effect cannot be explained by a broadening of islands sizes, and should be connected with the charge in the islands.

To understand the reason for this dependence, we suppose that hole emission from QW islands (measured by DLTS) takes place via a two-step process. The first step is the emission from the island to the wetting layer, and the second step is the emission from the wetting layer to the silicon layer. But, if the hole concentration in the islands becomes so large as to produce a strong electric field around the islands, hole emission from the islands to the wetting layer is enhanced due to thermally activated tunneling. Really, a charged island with disclike shape creates an electric field around itself, which is essentially stronger in the lateral direction (F_L) than in the perpendicular direction (F_Z), if the height of the islands $d \ll D$, where D is the characteristic diameter of the island in the QW layer (xy plane) (Fig. 9).

One can get $F_L/F_Z = D/d$ by using the formula for the potential distribution around a charged metallic ellipsoid with a large difference between the z and x/y dimensions.[19] This approximation leads to the following relation

$$F_L = \frac{Q}{\pi \varepsilon_0 \varepsilon_r d D} = \frac{e n_{dw} D}{4 \varepsilon_0 \varepsilon_r d}, \tag{2}$$

where n_{dw} is the average surface charge of the islands, and $\varepsilon_0 \varepsilon_r$ is dielectric constant in the wetting layer. For the Ge-rich islands of the investigated structures, D/d is about 30 (Table I). The strong electric field induced by charge in the island should enhance hole emission from the island to the wetting layer. The enhancement of the hole emission rate from QW due to thermally activated tunneling induced by electric field was analyzed in Ref. 15. We apply the same approach to the thermally activated tunneling from islands to wetting layer, which results in the dependence[15]

$$e_T = e_{T0} \exp\left(\frac{F_L^2}{F_c^2}\right), \tag{3}$$

where the characteristic field F_c is given by

$$F_c^2 = \frac{24 m^* (k_B T)^3}{\hbar^2 e^2}, \tag{4}$$

and e_{T0} is the emission rate in the absence of electric field, and m^* is the effective hole mass. Correspondingly, the effective activation energy E_a^* of the emission rate from an island to the wetting layer is given as function of the dot-hole concentration n_{dw}

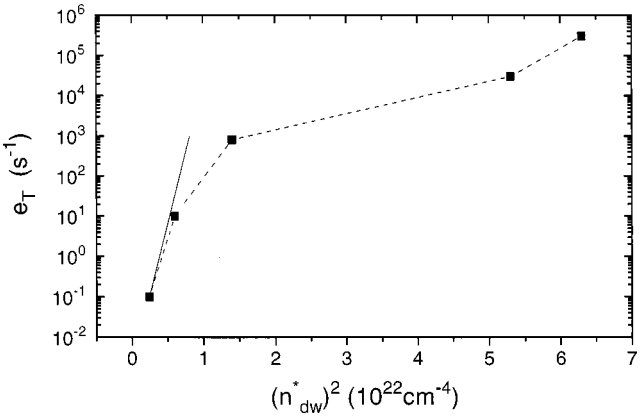

FIG. 10. Hole emission rate e_T as a function of the quadratic hole concentration n_{dw} in the islands for p-type Si/Ge/Si structure with 12 ML Ge deposition (dashed line—experimental data, straight line—theoretical dependence).

$$E_a^* = (E_{vd} - E_{vw}) - (E_{1d} - E_{1w}) - k_B T \left(\frac{n_{dw}}{n_c}\right)^2, \tag{5}$$

where $(E_{vd} - E_{vw})$ is the band offset between the Ge-rich island and the wetting layer, and $(E_{1d} - E_{1w})$ is the difference in the respective space quantization energies. The characteristic concentration n_c depends strongly on temperature

$$n_c = \frac{8\sqrt{6}\varepsilon_0 \varepsilon_r (m^*)^{1/2} (k_B T)^{3/2}}{e^2 \hbar} \left(\frac{d}{D}\right). \tag{6}$$

An estimation based on Eq. (6) with parameters of pure Ge [$m^* = 0.043 m_0$ (light-hole mass), $\varepsilon_r = 16$] gives $n_c = 0.25 \times 10^{11}\,\mathrm{cm}^{-2}$ at $T = 67\,\mathrm{K}$. An estimation of the hole concentration n_{dw} in an island for the investigated samples by using Eq. (1) shows that n_{dw} becomes really larger than the critical concentration n_c. Thus, the condition for lateral thermally activated tunneling is realized.

In Fig. 10, the experimental dependence of the hole emission rate e_T is presented as a function of the quadratic average concentration $(n_{dw})^2$ in the islands. The dependence (for the 12-ML structure) of e_T on the activation energy E_a was obtained from Fig. 7 at 100 K (for few points by extrapolation). The dependence n_{dw} versus E_a was calculated from the experimental data in Fig. 8 using Eq. (1). In Fig. 10, the theoretical dependence according to Eq. (6) with the characteristic concentration $n_c = 0.25^* 10^{11}\,\mathrm{cm}^{-2}$ is also shown. The experimental results for low-hole concentrations, i.e., when all confined holes are practically localized in the islands, are well approximated by the theoretical dependence. But, at larger hole concentrations the hole emission rate appears to be controlled by the hole emission from the wetting layer, and therefore the dependence of the hole emission rate on the hole concentration is essentially weaker.

V. CONCLUSIONS

In conclusion, we have demonstrated the effect of lateral thermally activated tunneling of confined holes from Ge-rich islands to the wetting layer in Si/Ge/Si structures. This effect is related to the Coulomb charge accumulated in the islands.

For disc-shaped islands, the lateral electric field is essentially larger than the perpendicular electric field, leading to an effective lateral tunneling of holes. The induced lateral transport of holes should play an essential role in the operation of optoelectronic devices based on quantum semiconductor structures containing layers with dots (islands).

ACKNOWLEDGMENTS

We are indebted to A. Ourmazd for a critical reading and useful comments. We acknowledge the support of the Volkswagen-Stiftung. We would like to express our gratitude to R. Winkler for technical assistance.

[1] D. Leonard, M. Krishnamurthy, C. M. Reaves, S. P. Den Baars, and P. M. Petroff, Appl. Phys. Lett. **63**, 3203 (1993).
[2] J. Ahopelto, A. A. Yamaguchi, K. Nishi, A. Usui, and H. Sakkai, Jpn. J. Appl. Phys., Part 1 **32**, 132 (1993).
[3] F. Hatami, N. N. Ledentsov, M. Grundmann, J. Böhrer, F. Heinrichsdorff, M. Beer, S. S. Ruvimov, P. Werner, U. Gösele, J. Heydenreich, U. Richter, S. V. Ivanov, B. Y. Meltser, P. S. Kopev, and Z. I. Alferov, Appl. Phys. Lett. **67**, 656 (1995).
[4] J. Eaglesham and M. Cerullo, Phys. Rev. Lett. **64**, 1943 (1990).
[5] W. Mo, D. E. Savage, B. S. Swartzentruber, and M. G. Lagally, Phys. Rev. Lett. **65**, 1020 (1990).
[6] O. Hansson, M. Albrecht, H. P. Strunk, E. Bauser, and J. H. Werner, Thin Solid Films **216**, 199 (1992).
[7] H. Sunamura, Y. Shiraki, and S. Fukatsu, Appl. Phys. Lett. **66**, 953 (1995).
[8] P. Schittenhelm, M. Gail, J. Brunner, J. F. Nützel, and G. Abstreiter, Appl. Phys. Lett. **67**, 1292 (1995).
[9] P. Schittenhelm, M. Gail, and G. Abstreiter, J. Cryst. Growth **157**, 260 (1995).
[10] G. Abstreiter, P. Schittenhelm, C. Engel, E. Silveira, A. Zrenner, D. Meertens, and W. Jäger, Semicond. Sci. Technol. **11**, 1521 (1996).
[11] P. Schittenhelm, G. Abstreiter, A. Darhuber, G. Bauer, A. Kosogov, and P. Werner, Thin Solid Films (to be published).
[12] R. Apetz, L. Vescan, A. Hartmann, C. Dieker, and H. Lüth, Appl. Phys. Lett. **66**, 445 (1995).
[13] H. Petterson, S. Anand, H. G. Grimmeiss, and L. Samuelson, Phys. Rev. B **53**, R10 497 (1996).
[14] K. Schmalz, I. N. Yassievich, H. Rücker, H. G. Grimmeiss, H. Frankenfeld, W. Mehr, H. J. Osten, P. Schley, and H. P. Zeindl, Phys. Rev. B **50**, 14 287 (1994).
[15] K. Schmalz, I. N. Yassievich, E. J. Collart, and D. J. Gravensteijn, Phys. Rev. B **54**, 16 799 (1996).
[16] O. Chretien, R. Apetz, L. Vescan, A. Souifi, H. Lüth, K. Schmalz, and J. J. Koulman, J. Appl. Phys. **78**, 5439 (1995).
[17] D. Vuillaume, J. C. Bourgoin, and M. Lannoo, Phys. Rev. B **34**, 1171 (1986).
[18] M. V. Belousov, N. N. Ledentsov, M. V. Maximov, P. D. Wang, I. N. Yassievich, N. N. Faleev, I. A. Kozin, V. M. Ustinov, P. S. Kop'ev, and C. M. Sotomayor Torres, Phys. Rev. B **51**, 14 346 (1995).
[19] E. D. Landau and M. F. Lifschitz, *Elektrodynamik der Kontinua* (Akademieverlag, Berlin, 1985).